

Crystal Growth of Single Salicylamide Crystals

Aisling Lynch, and Åke C. Rasmuson

Cryst. Growth Des., **Just Accepted Manuscript** • DOI: 10.1021/acs.cgd.9b01101 • Publication Date (Web): 21 Oct 2019

Downloaded from pubs.acs.org on October 29, 2019

Just Accepted

“Just Accepted” manuscripts have been peer-reviewed and accepted for publication. They are posted online prior to technical editing, formatting for publication and author proofing. The American Chemical Society provides “Just Accepted” as a service to the research community to expedite the dissemination of scientific material as soon as possible after acceptance. “Just Accepted” manuscripts appear in full in PDF format accompanied by an HTML abstract. “Just Accepted” manuscripts have been fully peer reviewed, but should not be considered the official version of record. They are citable by the Digital Object Identifier (DOI®). “Just Accepted” is an optional service offered to authors. Therefore, the “Just Accepted” Web site may not include all articles that will be published in the journal. After a manuscript is technically edited and formatted, it will be removed from the “Just Accepted” Web site and published as an ASAP article. Note that technical editing may introduce minor changes to the manuscript text and/or graphics which could affect content, and all legal disclaimers and ethical guidelines that apply to the journal pertain. ACS cannot be held responsible for errors or consequences arising from the use of information contained in these “Just Accepted” manuscripts.

Cover Page

Crystal Growth of Single Salicylamide Crystals

Lynch Aisling¹, Rasmuson Åke*^{1 2}

¹Synthesis and Solid State Pharmaceutical Centre, Materials and Surface Science Institute, Department of Chemical and Environmental Science, University of Limerick, Limerick (Ireland)

²Department of Chemical Engineering and Technology, KTH Royal Institute of Technology, SE-100 44 Stockholm (Sweden)

*email: Ake.Rasmuson@ul.ie

Growth of single salicylamide crystals has been investigated in a non-stirred growth cuvette and on a rotating disk. In the growth cuvette the crystal growth rates were measured for both primary nucleated crystals and seed crystals manually inserted into the cuvette. In the rotating disk experiments multiple seed crystals were attached to a disk that was rotated in a supersaturated solution. The crystal growth rates in the length and width direction were precisely measured *in-situ* for each individual crystal; and growth rates were also extracted for a specific crystal facet i.e. (200). In all cases, the growth rate was considerably faster in the rotating disk experiments, shown to be governed by surface integration. Solvent was found to impact the growth rates of the crystal facets in part by creating different surface features. The influence of the supersaturation on the crystal growth rate depended on the solvent, in general an increasing trend was observed. At relatively low supersaturations, it was discovered that the growth process will focus on repairing morphological defects. Within the range of experimental conditions, the growth kinetics were strongly affected by the temperature as was further indicated by the relatively high activation energy values obtained. The crystal seed quality was found to have a substantial impact on the growth rate, with rougher crystals leading to quicker growth. A wide growth rate dispersion was obtained for both crystal growth methods, found to be reduced by using seed crystals with high quality, lower supersaturations and also within certain solvents.

1
2
3
4 305
6 317
8
9 3210
11 33 Åke C. Rasmuson12
13
14 34 Department of Chemical and Environmental Science,15
16 35 University of Limerick,17
18 36 Limerick (Ireland)19
20
21 37 Email: ake.rasmuson@ul.ie22
23 38 Tel: +353 61 23461724
25
26 39

Title Page

27
28
29
30
31
32 40

Crystal Growth of Single Salicylamide Crystals

33
34
35 41

Lynch Aisling¹, Rasmuson Åke^{1 2}*

36
37 42 ¹Synthesis and Solid State Pharmaceutical Centre, Materials and Surface Science Institute, Department of
38 43 Chemical and Environmental Science, University of Limerick, Limerick (Ireland)39
40 44 ²Department of Chemical Engineering and Technology, KTH Royal Institute of Technology, SE-100 44
41 45 Stockholm (Sweden)42
43 46 *email: Ake.Rasmuson@ul.ie44
45
46 47

Abstract

47
48
49
50 49 Growth of single salicylamide crystals has been investigated in a non-stirred growth
51 50 cuvette and on a rotating disk. In the growth cuvette the crystal growth rates were
52 51 measured for both primary nucleated crystals and seed crystals manually inserted into
53 52 the cuvette. In the rotating disk experiments multiple seed crystals were attached to a
54 53 disk that was rotated in a supersaturated solution. The crystal growth rates in the length

1
2
3
4 54 and width direction were precisely measured *in-situ* for each individual crystal; and
5
6 55 growth rates were also extracted for a specific crystal facet i.e. (200). In all cases, the
7
8 56 growth rate was considerably faster in the rotating disk experiments, shown to be
9
10 57 governed by surface integration. Solvent was found to impact the growth rates of the crystal
11
12 58 facets in part by creating different surface features. The influence of the supersaturation on
13
14 59 the crystal growth rate depended on the solvent, in general an increasing trend was
15
16 60 observed. At relatively low supersaturations, it was discovered that the growth
17
18 61 process will focus on repairing morphological defects. Within the range of experimental
19
20 62 conditions, the growth kinetics were strongly affected by the temperature as was further
21
22 63 indicated by the relatively high activation energy values obtained. The crystal seed quality
23
24 64 was found to have a substantial impact on the growth rate, with rougher crystals leading
25
26 65 to quicker growth. A wide growth rate dispersion was obtained for both crystal growth
27
28 66 methods, found to be reduced by using seed crystals with high quality, lower
29
30 67 supersaturations and also within certain solvents.

31
32
33 68

34
35
36
37 69 **Keywords:** Crystal Growth Kinetics, Diffusion Control, Surface Integration Control,
38
39
40
41 70 Rotating Disk Method, Solvent Effect, Morphology, Individual Facets, Growth
42
43
44 71 Mechanism.

72 Introduction

73 Crystallisation is a very important technique, especially in the pharmaceutical industry,
74 as it is used in the formation, purification and recovery of the majority of active
75 pharmaceutical ingredients (API) ¹⁻². Crystallisation is a two-step process: initial
76 nucleation followed by subsequent crystal growth. Presently, crystallization fundamentals
77 of both steps are still insufficiently understood, and the crystal growth kinetic data can differ by
78 an order of magnitude for the same API depending on the laboratory generating the data.
79 Literature depicts many ways in which the crystal growth process can be observed and associated
80 growth rates measured dependent on the crystal growth method used ³⁻¹⁴. These methods can be
81 split into either single crystal growth or multiple crystal growth, the basic difference being that
82 in the first type of method the actual growth rate of the individual crystal is recorded while in the
83 second type the average growth rate of an ensemble of crystals is determined without
84 distinguishing the growth of each individual crystal. An advantage of single crystal growth
85 methods is that the detailed growth in different directions and of different faces can be measured
86 ^{2, 15}. However, the hydrodynamic conditions that can be used are restricted and often far from
87 those in a real crystallizer. Benefits of the multiple crystal growth methods is that a better
88 statistical averaging can be obtained and the hydrodynamic conditions can resemble industrial
89 conditions.

90 There have been surprisingly limited kinetic studies on the growth of the individual faces of
91 spontaneously-nucleated crystals grown in stagnant solutions. Recent work by Nguyen studied
92 the influence of solvent on the growth rate of ibuprofen crystal facets and overall crystal habit
93 using a stagnant solution in a cuvette ¹⁴. Such measurements are helpful in that they provide
94 baseline crystal growth kinetic data from which the impact of e.g. seeds, agitation and mixing
95 can be assessed subsequently. Since the 1970's researches have made attempts at introducing
96 mixing of the solution into single crystal growth experiments in order to control the
97 hydrodynamics. The most successful was a simple closed flow cell combined with an optical
98 microscope to observe the growth of the (100) face of ammonium dihydrogen phosphate crystals
99 ¹⁰. Since then this single crystal growth method using liquid flow has been used by many to study
100 the growth rates of other compounds such as glycine, α and β polymorphs of L-glutamic acid ^{3,}
101 ^{5, 11, 16-17}. The issue with this flow design results in growth being unidirectional, so growth of the
102 crystal is not representative of a true crystal. In addition, it becomes very tedious to obtain
103 statistically valid data over a number of crystals. Rotating disks have also been used a few times
104 to study crystal growth in a mixed solution ¹⁸⁻¹⁹. However, they only studied the growth of one
105 compressed crystal plane. By using an agitated batch crystalliser combined with a high speed
106 camera it has been shown to be possible to measure the growth rates of either the length and
107 width or facet direction for a number of individual crystals grown at once ^{13, 20-21}. The
108 disadvantage of this analysis is that the growth of a specific crystal can't be tracked, rather results
109 are averages of the whole crystal population.

1
2
3 110 A similar approach to the work of Nguyen will be used in our study to determine the growth
4
5 111 rates of single salicylamide crystals in a stagnant solution in a cuvette. Furthermore, an
6
7 112 alternative multiple single crystal growth method has been developed where the
8
9 113 hydrodynamic environment is controlled by attaching a number of seed crystals to a
10
11 114 rotating disk, yet can also track multiple single crystals for their specific facet growth
12
13 115 rates at once. Salicylamide's properties including its chemical, uses, classification, and
14
15 116 solubility have already been described in detail ²²⁻²⁴. The pharmaceutical industry is also
16
17 117 interested in how the process conditions such as temperature, solvent, supersaturation,
18
19 118 and seed quality effect the crystal growth kinetics and so these have been investigated
20
21 119 in this study ^{2, 14, 25-27}.

1
2
3
4 120 **Experimental**
5
6

7
8 121 *Materials*
9

10 122 The solute (salicylamide, SAM) and the solvents (acetone, AC, acetonitrile, MeCN, ethyl
11 acetate, EA, and methanol, MeOH) all had purity $\geq 99.0\%$. All were purchased from
12 123 Sigma Aldrich and used as received.
13
14 124
15

16
17 125

18 126 *Seed Crystal Preparation*
19

20
21 127 Salicylamide was supplied as crystalline material, the polymorphic form of which was
22 confirmed by P-XRD (PANalytical Empyrean X-Ray diffractometer) and found to be the
23 128 required stable form so was deemed suitable for use without the need for
24 129 recrystallization. Crystals were sieved using fisherbrand stainless steel woven wire
25 130 mesh test sieve with a 300-355 μm aperture; the resulting sieve fraction was used as
26 131 the seed crystals in both crystal growth methods.
27
28
29
30
31
32

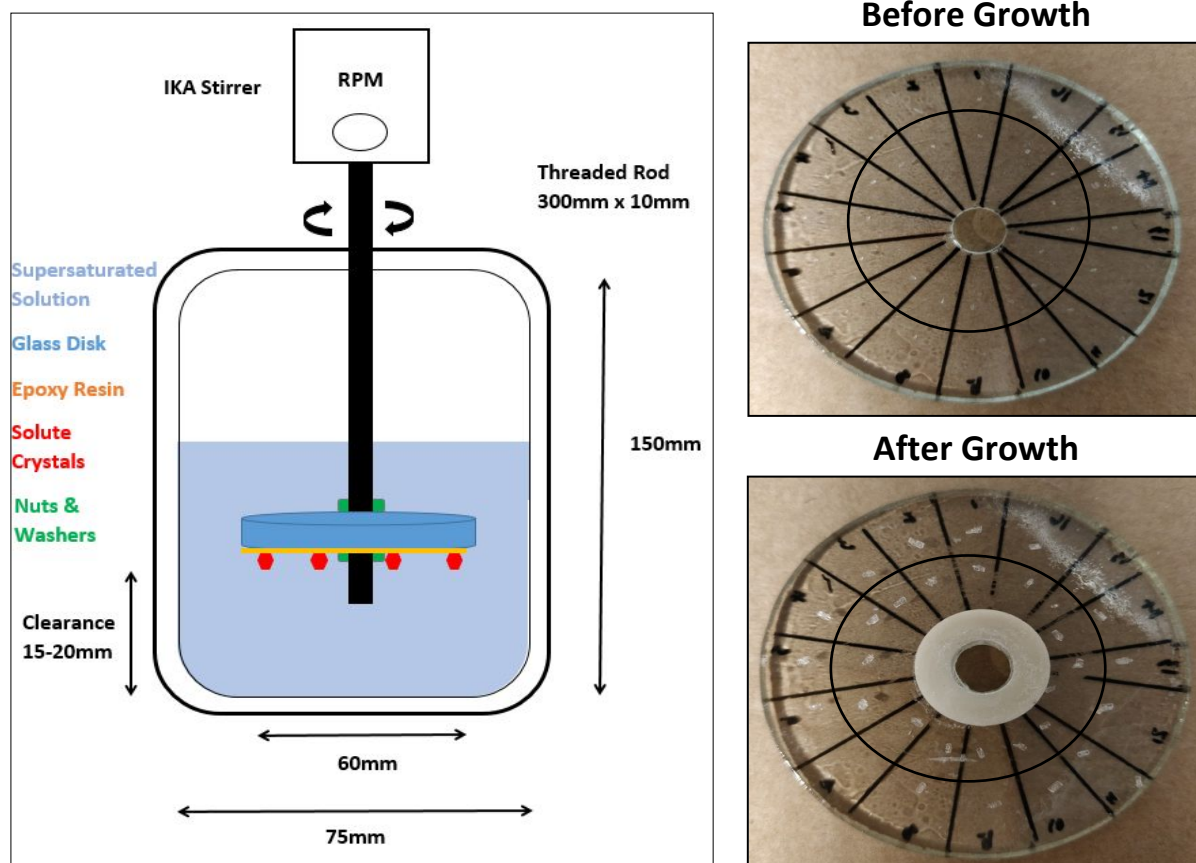
33
34 133

35 134 *Cuvette growth experiments*
36

37
38 135 A spectrophotometer cuvette 0.4 mL (55 x 10 x 1 mm, Starna Cells 21-SOG-1) was
39 used as a growth vessel. Both the growth of seed crystals (sieve fraction 300-355 μm) and
40 136 also spontaneous nucleated crystals were studied under stagnant growth. At the start,
41 137 crystal seeds were either mechanically placed inside the cuvette before the start of the
42 138 growth experiments or they were generated by primary nucleation *in-situ* in the cuvette.
43
44 139 For both crystal types, the cuvette was filled with supersaturated solution; which was
45 prepared by dissolving excess solute in solvent with sufficient mixing for minimum 1 hr
46 140 and then let to settle and filtered with a 0.2 μm filter. This cuvette was placed into a
47 shallow closed tank of water connected to a circulator (Lauda ECO Silver, RE415) to
48 141 control the growth temperature at 15 °C and placed onto the microscope stage. Crystals
49 were allowed to grow for 1 hr, with micrographs captured at either 1 or 10 min intervals
50
51
52
53
54
55
56
57
58
59
60

1
2
3
4 146 using the optical microscope. The spontaneously nucleated crystal growth experiments
5
6 147 used a relatively higher supersaturation, $S-1$ in the range of 0.24 – 0.89, than compared
7
8 148 with the seed crystal growth experiments, $S-1$ in the range of 0.02 – 0.12, to induce
9
10 149 spontaneous nucleation. The growth of a minimum of 5 crystals was determined for
11
12 150 each condition, so that an average of the growth rates could be calculated. Crystal
13
14 151 growth of both single crystal types were studied in four solvents (AC, MeCN, EA or
15
16 152 MeOH). Also, each crystal type was studied under two different supersaturations per
17
18 153 each solvent. The crystal increased in size for the first 2 to 10 min for spontaneously nucleated
19
20 154 crystals and 30 min to 60 min for seed crystals but then began to plateau as surrounding solution
21
22 155 became saturated.

23
24
25
26
27
28
29
30
31
32
33
34
35
36
37
38
39
40
41
42
43
44
45
46
47
48
49
50
51
52
53
54
55
56
57
58
59
60



157 *Rotating disk growth experiments*

158 **Figure 1.** Schematic for the apparatus set-up for single crystal growth studies using a rotating
 159 disk. Glass disk has diameter 60 mm, and hole in center, for stirrer, is 10 mm.

160 A jacketed 500 mL glass reactor with inner diameter of 75 mm and a rotating 60 mm
 161 glass disk, as shown in Figure 1 was used as the growth vessel. Reactor was kept at a
 162 constant crystal growth temperature by using a circulator (Lauda, RE305 series). A total
 163 of 32 crystals of sieve fraction 300 - 355 μm were attached evenly onto the glass disk
 164 using a thin layer of epoxy resin, and allowed to set for a minimum of three hours at 40
 165 $^{\circ}\text{C}$. Crystals were orientated in such a way so that they were lying flat on the disk with
 166 their largest facet facing upwards, they were gently placed on top of the glue so they
 167 did not become embedded within the resin which allowed both the top and side facets
 168 of the crystals to grow. Slightly supersaturated solution was prepared in the reactor by
 169 adding a known amount of excess solute to 200 mL of solvent and let to mix at 250 rpm
 170 using a 60 mm 4-pitched-blade PTFE coated impeller with inclined blades at 6 $^{\circ}\text{C}$ above

1
2
3
4 171 crystal growth temperature for 20 min. Reactor temperature was then decreased to
5
6 172 required growth temperature, and allowed to stabilise for a further 20 min. Impeller blade
7
8 173 was removed and replaced with a 316 stainless steel rod which had the glass disk (with
9
10 174 crystals) attached using steel nut and washers. Disk was left rotating at 200 rpm for a
11
12 175 growth period of 1 hr. Micrographs of each crystal were captured before and after the
13
14 176 growth period using an optical microscope. Crystal growth rate of single crystals were
15
16 177 studied at 15 °C in four different solvents (AC, MeCN, EA or MeOH) and at different
17
18 178 supersaturations ($S-1$ of 0.007 - 0.05). In acetonitrile also the influence of temperature
19
20 179 was investigated by additional experiments at 10 and 20 °C. Growth rates for each of
21
22 180 the 32 crystals were calculated and also the average growth rate of all the crystals grown
23
24 181 in one system. To ensure that decay of supersaturation concentration was negligible
25
26 182 throughout the growth period the concentration decay was measured experimentally
27
28 183 and found to be <3 % i.e. maximum supersaturation decay would result in an initial
29
30 184 supersaturation of 0.030 decreasing to 0.029 after the 1 hr growth time [refer to
31
32 185 supplementary section for outline of these calculations].

33
34 186 Certain experimental variables were trialled to determine the optimum parameters for the rotating
35
36 187 disk experiments which are defined above. The variables that were tested included the overall
37
38 188 number of crystals attached on the disk (32 vs. 48) plus their respective position and also the
39
40 189 growth time (10 min up to 2 hr). Also the method was repeated three times using the same
41
42 190 conditions to determine reproducibility of experiments and proved successful (average growth
43
44 191 rate of length was $0.28 \pm 0.02 \mu\text{m/s}$). Results of all of these trial studies can be found in the
45
46 192 supplementary section.

47 193 *Measuring crystal growth rate*

48 194 For both of the single crystal growth experiments, micrographs of the crystals were captured
49
50 195 using an inverted light optical microscope (Olympus IX53) integrated with Olympus SC100
51
52 196 camera. The size of the crystal in a certain dimension at each time point was measured directly
53
54 197 from these micrographs using the image/ video capture and analysis software (Olympus Stream
55
56 198 Essentials). Measurements were taken in both the length & width (maximum and minimum feret
57
58 199 diameter respectively) direction and more precisely the miller indexed (200) face for SAM (as
59
60 200 illustrated in Figure 3). Example of the micrographs and measurements taken at different
201
202 stages during the growth period are shown in Figure 2. In this case, the (200) face was
equivalent to the width measurements divided by two. It is worth noting from Figure 3 that

measuring the growth of SAM in the width direction is not always representative of the same crystal facet. For the SAM crystal shown on the left, the width represents the (200) face, whereas for the SAM crystal on the right hand side the length represents the (200) face. This causes issues when reporting growth rates in terms of length and width for SAM as it can lead to potentially larger GRD due to measuring growth of different faces. This highlights the importance of reporting growth rates for crystal facets rather than just directions.

The crystal growth rate of the crystal is determined by plotting the size of the crystal versus the time and obtaining the slope of the line i.e. the growth rate in specific direction, G (μms^{-1})

$$G = dL/dt \quad (1)$$

Where G is the rate of change of the crystal's characteristic dimension, L , has dimensions of velocity with respect to time, t .

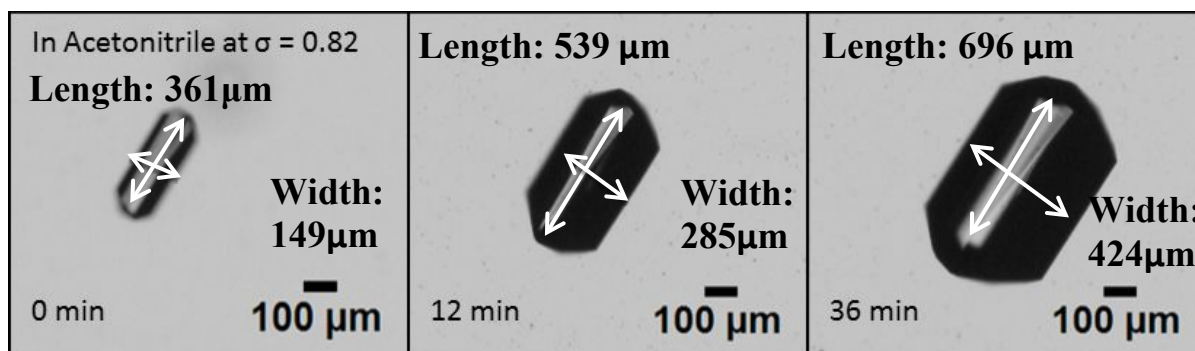


Figure 2. Series of micrographs of salicylamide crystals grown by the cuvette growth method using spontaneous nucleation in acetonitrile using S-1 of 0.82 at crystal growth temperature of 15 °C as a function of growth time.

219

220

221

222

223

224

225

226

227

228

229

230

231

232

233

234

235

236

237

238

239

240

241

242

243

244

245

246

247

248

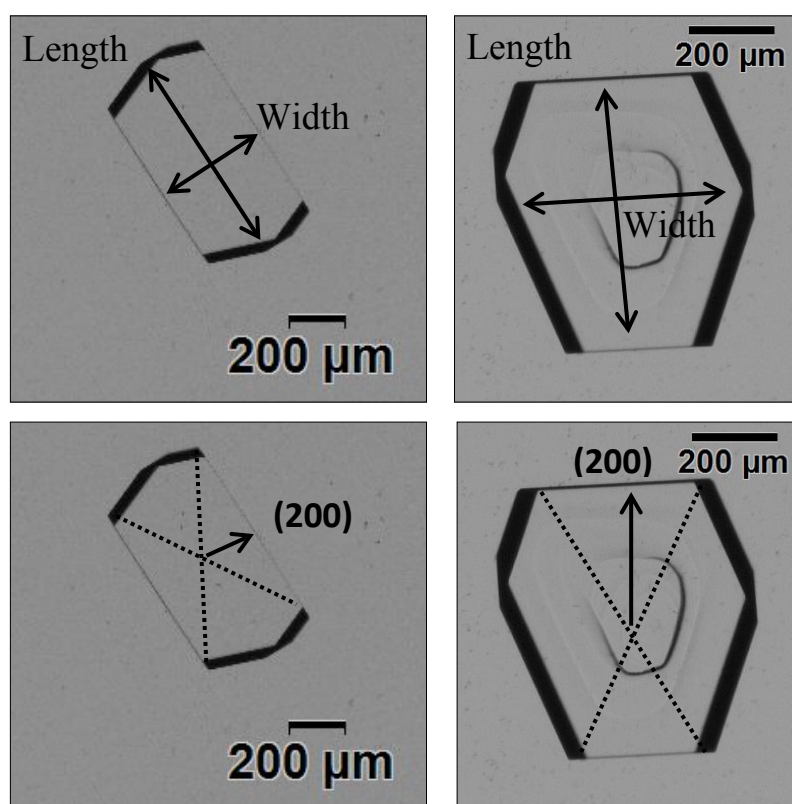


Figure 3.

Micrographs during single growth studies, length and also (200) face of salicylamide

taken crystal with width and identified crystals,

for rectangle plate and block habit respectively.

Crystal surface analysis

The surface of the SAM crystals was analysed using a scanning electron microscopy (SEM), Carry Scope JEOL JCM-5700. Prior to visualisation with the SEM the crystal samples were gold coated with 20 mA for a maximum of one minute.

1
2
3
4 249 **Results and Discussion**

5
6 250 Cuvette growth experiments

7
8
9 251 *Habit*

10
11 252 Individual spontaneously nucleated crystals and seed crystals grown in a stagnant solution in
12 253 each of the four solvents under different supersaturations are shown in Figure 4. Under certain
13 254 conditions, spontaneously nucleated crystals and seed crystals can grow to a maximum width of
14 255 500 μm and 850 μm respectively. Seed crystals grew 2.5 times the size in width direction and 5
15 256 times the size in the length direction at certain conditions (850 x 1700 μm). For crystals that were
16 257 spontaneously nucleated as shown in the top two rows, the crystal habit differed depending on
17 258 the solvent and initial supersaturation. When crystals were formed and grown from acetone and
18 259 methanol, the rectangle crystal habit of salicylamide depended on the level of initial
19 260 supersaturation, while at the lower supersaturation less elongated particles were being observed.
20 261 On the other hand, in acetonitrile, regardless of the initial supersaturation, elongated rectangle
21 262 particles were formed. In ethyl acetate, the crystals formed irregular hexagonal plates regardless
22 263 of the initial supersaturation. This habit change has been discussed in detail in our previous work
23 264 where we also examined the underlying crystal structure of the main crystal facets of salicylamide
24 265 at a molecular level in attempt to understand the growth process³⁰. When performing similar
25 266 single crystal growth studies but using seed crystals as shown in the bottom two rows, the
26 267 influence of solvent on the crystal habit of salicylamide appears to be negligible. Instead, the
27 268 initial rectangular plate habit of the seed crystal was maintained throughout the growth period in
28 269 all four solvents.

29
30
31
32
33
34
35 270
36
37
38
39
40
41
42
43
44
45
46
47
48
49
50
51
52
53
54
55
56
57
58
59
60

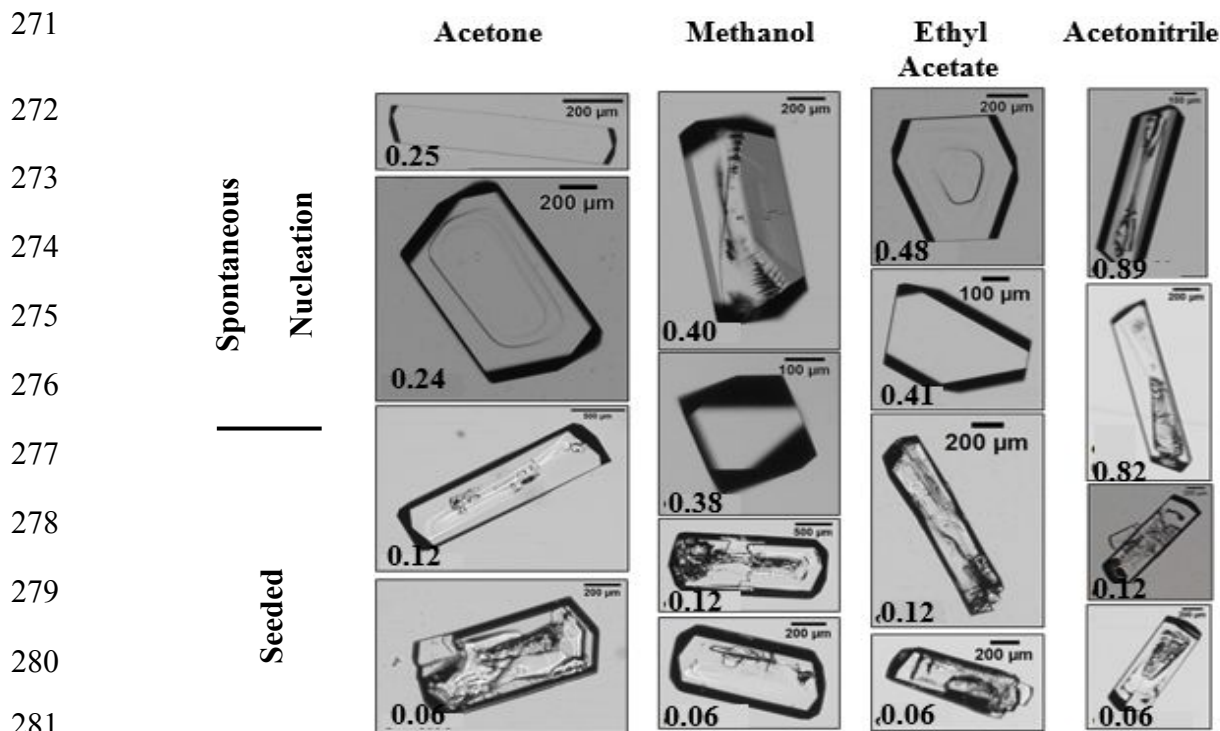


Figure 4. Micrographs of salicylamide crystals grown using the cuvette growth method at 15 °C. The top two rows refer to spontaneously nucleated crystals whereas the bottom two rows refer to the seed crystals. For both crystal types, micrographs are shown for each of the four solvents, under different supersaturations (the S-1 value is shown in the bottom left hand corner of each image, and ranges from 0.89 to 0.06). The crystals displayed here represent the dominant habit obtained in each condition, when each condition was repeated for a minimum of five crystals.

Kinetics – Effect of Solvent and Supersaturation

The average crystal growth rate of spontaneously nucleated and seed salicylamide crystals, as a function of solvent and supersaturation, is similar for length and width as shown in Figure 5. Growth rate of the length direction is faster than the growth rate of width direction of crystals at all conditions, by a minimum factor of 2. The average growth rate ratio of length to width increased with increasing supersaturation value for spontaneously nucleated crystals, whereas the ratio decreased with increasing supersaturation for seed crystals as shown in Figure 5 (e, f). In other words, spontaneously nucleated crystals grow at a similar rate in either dimension under the two supersaturations tested. Whereas seed crystals grow differently in the length and width dimensions depending on the supersaturation used; crystals grow proportionally faster in the width dimension than in the length at the higher driving force. The growth process of salicylamide was most strongly effected by change in driving force when EA was used as the solvent. The growth rate was found to vary not only from one condition to another, but also among the crystals grown in the same condition, this phenomenon being referred to as growth rate dispersion (GRD)¹⁴. GRD is observed at all conditions, the widest example is in EA at supersaturation 0.48 which used nucleation to form the crystal: from 0.1 μm/s up to 4.3 μm/s among the 5 crystals, see Figure 5 (a). The growth rate dispersion appears to increase with

1
2
3 306 increasing supersaturation in most of the solvents, and was higher for the spontaneously
4 307 nucleated crystals. There was a significantly narrower growth rate dispersion among the seed
5 308 crystals. In spite of the fairly strong GRD the influence of the supersaturation on the average
6 309 growth rate in all cases meets the expectation, i.e. the growth rate increases with increasing
7 310 supersaturation. However, the GRD is so significant that the evaluation of the influence of the
8 311 solvent should only be taken as indicative.

11
12 312 The growth rates of salicylamide crystals growing in the cuvette are considerably influenced by
13 313 the initial supersaturation as illustrated in Figure 5. In the experiments with spontaneously
14 314 nucleated crystals, the driving forces are set to induce nucleation, and hence is different in the
15 315 different solvents and an assessment of the actual influence of the solvent itself cannot be made.
16 316 In the seeded experiments, the same initial supersaturation (S-1) of 0.12 and 0.06 was used in all
17 317 solvents. The order of average crystal growth rate, with respect to solvent, changes somewhat
18 318 with supersaturation. At high supersaturation (0.12) the average crystal growth rate of
19 319 salicylamide is the highest in acetone and the lowest in acetonitrile, with methanol and ethyl
20 320 acetate in between, for both the length and width direction. At the lower supersaturation (0.06)
21 321 the growth rate of SAM is still the highest in acetone in both directions, but the order among the
22 322 other three is less systematic as shown in Figure 5 (c) and (d). As the cuvette growth method
23 323 uses a non-stirred solution the growth rate is likely to be governed by the rate of diffusion through
24 324 the fluid surrounding each crystal, which in turn is inversely proportional to the viscosity of the
25 325 solution. Methanol has the highest viscosity (0.54 mPa.s at 25 °C), compared to acetone which
26 326 has the lowest viscosity of the four solvents (0.31 mPa.s at 25 °C)²⁸. Using the Wilke and Chang
27 327 method²⁹ for estimating the diffusivity, it ranks the solvents in the order AC> EA> MeCN>
28 328 MeOH, which is quite similar to the order of decreasing solubility (mol/L) and in turn equalling
29 329 the growth rate order of seed crystals AC>EA>MeOH>MeCN.

30
31
32
33
34
35
36
37 330
38
39
40
41
42
43
44
45
46
47
48
49
50
51
52
53
54
55
56
57
58
59
60

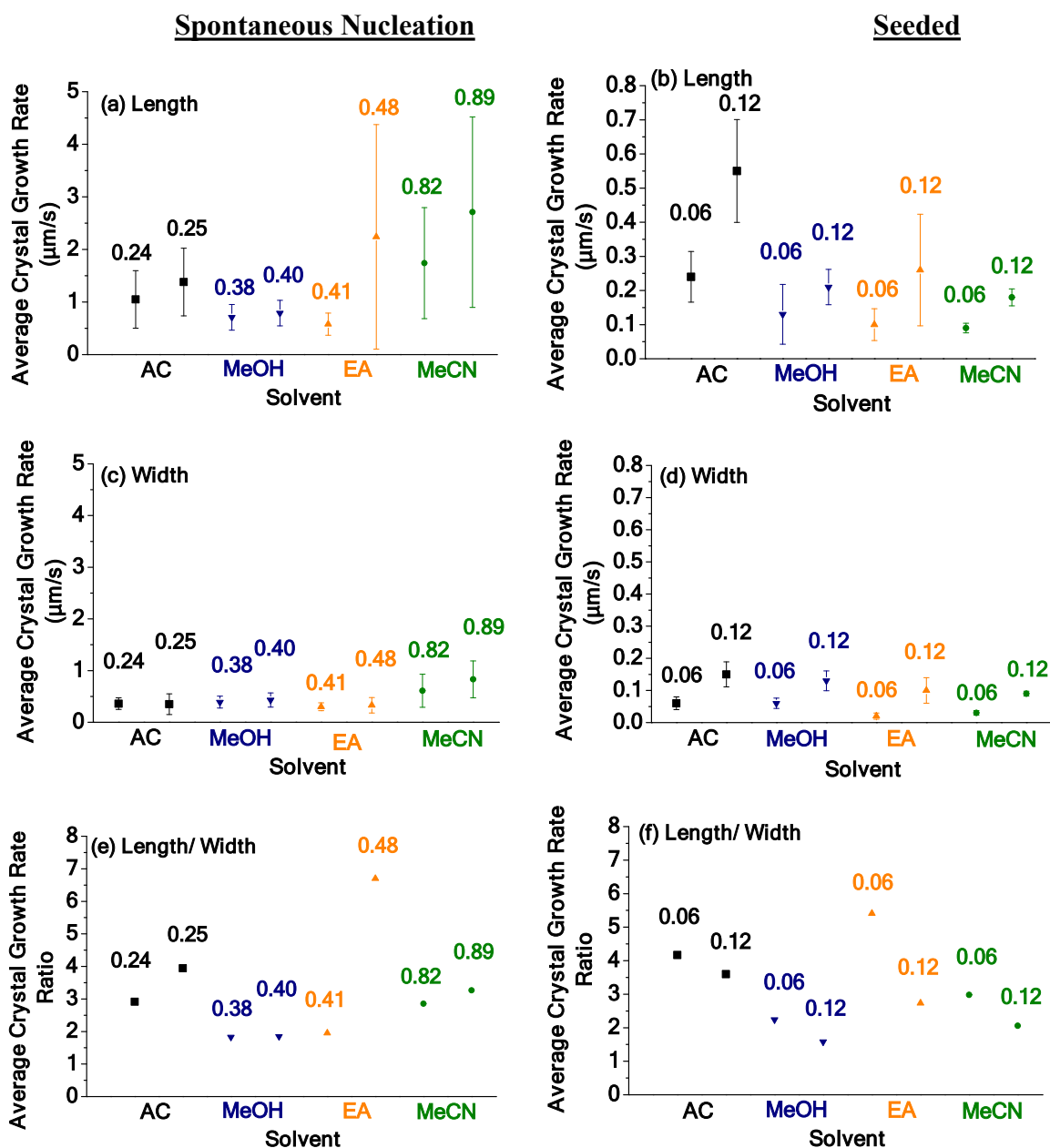
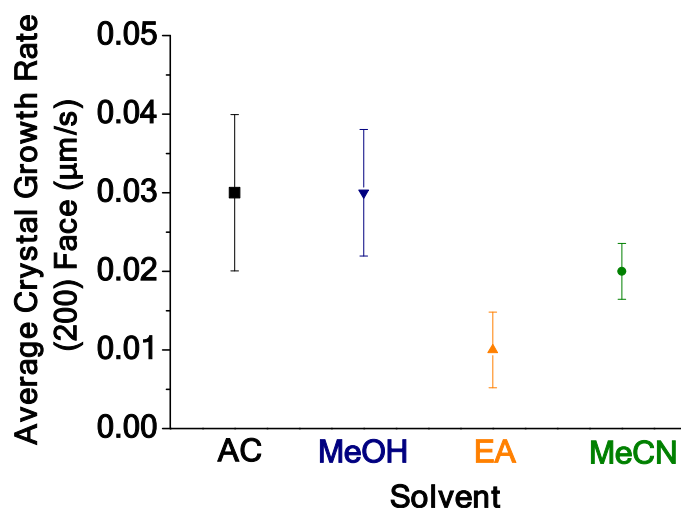


Figure 5. Average crystal growth rate ($\mu\text{m/s}$) of spontaneously nucleated (left) and seed (right) crystals in the length (a, b), width (c, d) direction and also average crystal growth rate ratio (e, f) as a function of solvent and supersaturation. Crystals are grown using the cuvette growth method at a growth temperature of $15\text{ }^\circ\text{C}$. Where AC is acetone, MeOH is methanol, EA is ethyl acetate and MeCN is acetonitrile; number above line is the supersaturation ($S-1$). The center point is the average crystal growth rate while the error bars on the graph illustrate the standard deviation of the data.

In our previous work we have face indexed experimentally grown salicylamide crystals using experimental and prediction techniques³⁰. All salicylamide crystals grown in these studies were flat plate-like crystals, indicating growth is stunted in one facet direction, this is the (002) face. The growth rate of this face is not measured in this study, since it appears perpendicular to the direction of observation. A mix of three end faces (-112), (011), and (110) represent the length direction, however all three faces may not appear in each crystal and so are difficult to track between crystals. The width typically represents the growth of the (200) and (-200) faces; and as

1
2
3 348 the (200) face is consistent between crystals, Figure 6 shows the influence of the solvent on the
4
5 349 growth rate of this specific face. Growth rate of the (200) face is found to follow the order
6
7 350 of $AC \geq MeOH > MeCN > EA$ at a supersaturation (S-1) of 0.06. Growth of the (200) face
8
9 351 is slower in ethyl acetate than in the other 3 solvents. As previously stated, in the length
10
11 352 direction the growth rate of SAM in ethyl acetate is faster than SAM in acetonitrile. These
12
13 353 findings indicate that ethyl acetate provides the slowest growth of the (200) facet out of
14
15 354 the four solvents tested yet only the second slowest growth rates of the faces in the
16
17 355 length direction of the crystal. In other words not all faces of the salicylamide crystal
18
19 356 habit grew at equivalent rates in the same solvent. This in agreement with findings in the
20
21 357 literature that state solvents may accelerate, retard or even stop the further outgrowth of
22 358 individual crystal faces, sometimes producing a habit change³¹.



39 359
40 360 **Figure 6.** Average crystal growth rate of (200) face (µm/s) of seed crystals with respect
41
42 361 to four different solvents. Crystals are grown using the cuvette growth method at a growth
43
44 362 temperature of 15 °C and supersaturation (S-1) of 0.06. The center point is the average crystal
45 363 growth rate while the error bars on the graph illustrate the standard deviation of the data.

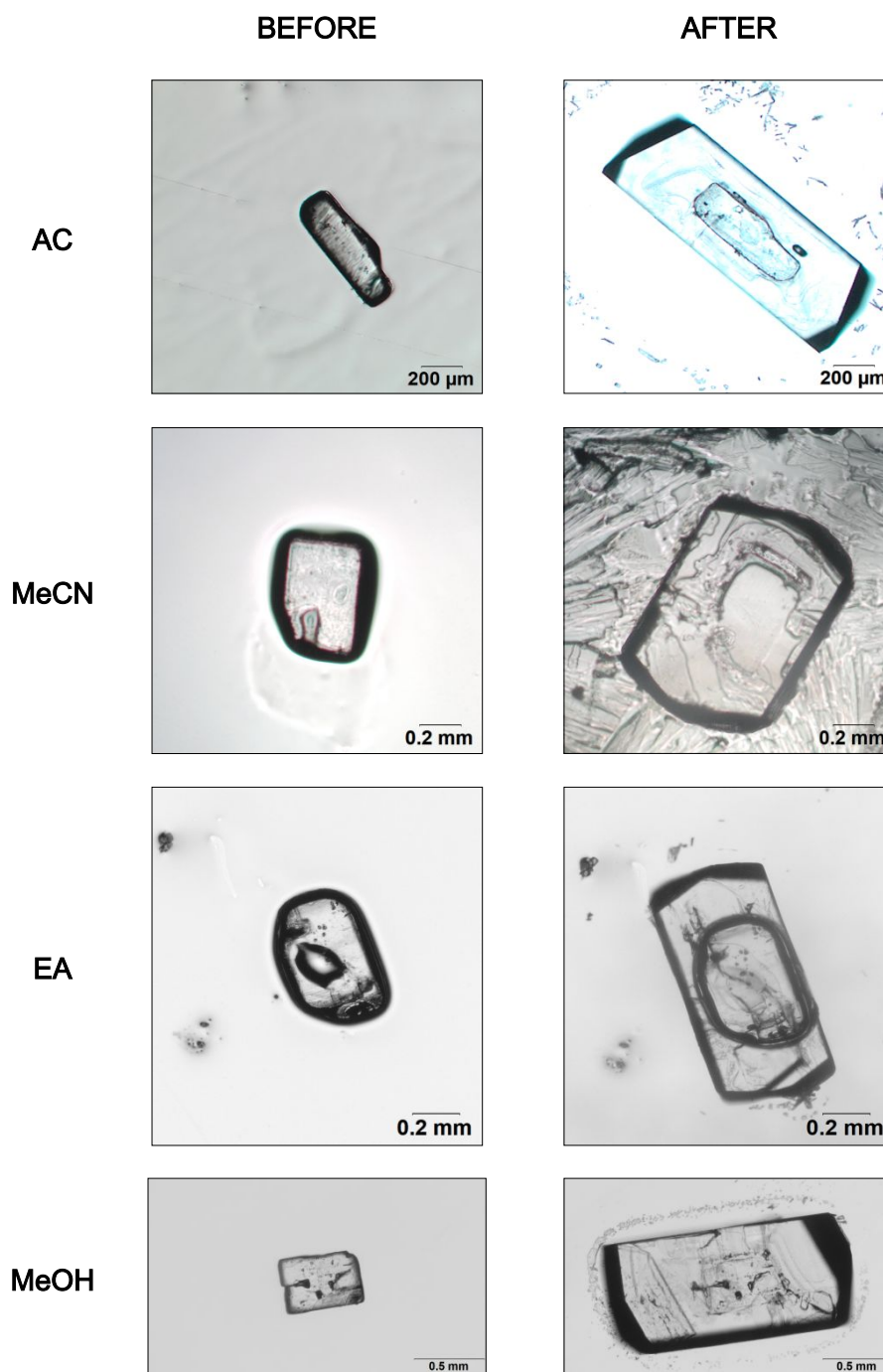
46
47 364

1
2
3
4 365 Rotating disk crystal growth

5
6 366 *Habit*

7
8
9 367 Micrographs taken before and after the growth of salicylamide crystals in the rotating
10
11 368 disk experiments are shown in Figure 7. The final habit appeared to be controlled by the
12
13 369 shape of the seed as was also found for similar seed crystals grown via the cuvette
14
15 370 crystal growth experiments. The outline of the seed is visible after growth in the final
16
17 371 crystal only because the crystals are opaque and fixed to the glass disk which makes
18
19 372 growth of that face rough.

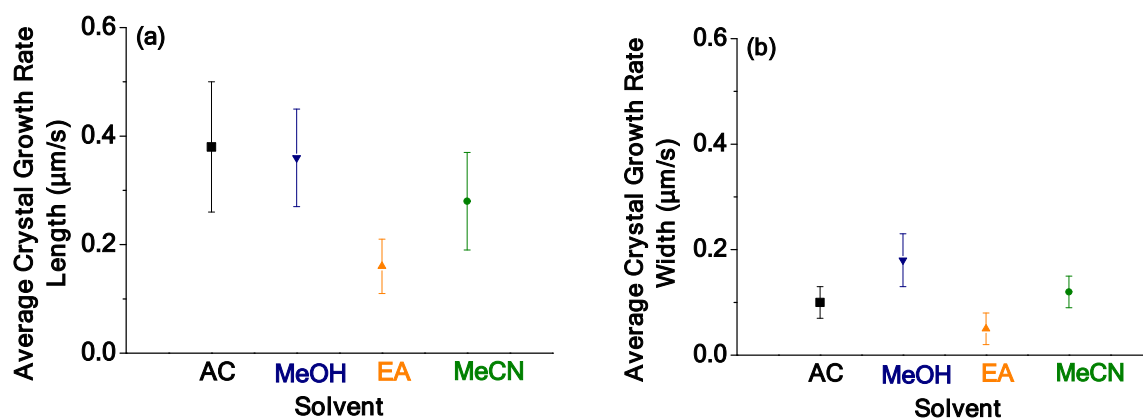
20
21
22 373
23
24
25
26
27
28
29
30
31
32
33
34
35
36
37
38
39
40
41
42
43
44
45
46
47
48
49
50
51
52
53
54
55
56
57
58
59
60



374 **Figure 7.** Micrographs of salicylamide crystals before and after crystal growth via the rotating
375 disk method. Salicylamide seed crystals are grown in each of the 4 solvents at growth
376 temperature of 15 °C under supersaturation (S-1) of 0.03 for 1 hr. Only one representative
377 crystal out of the total 32 crystals for each condition are shown for each in this image.

378 *Kinetics – Effect of Solvent*

379 There is little difference between the average growth rates of the seed crystals in the
 380 different solvents except for in EA when using a crystal growth temperature of 15 °C
 381 and supersaturation (S-1) of 0.03 as illustrated in Figure 8. In both the length and width
 382 directions ethyl acetate provides the slowest growth rates of salicylamide compared to
 383 the other solvents.



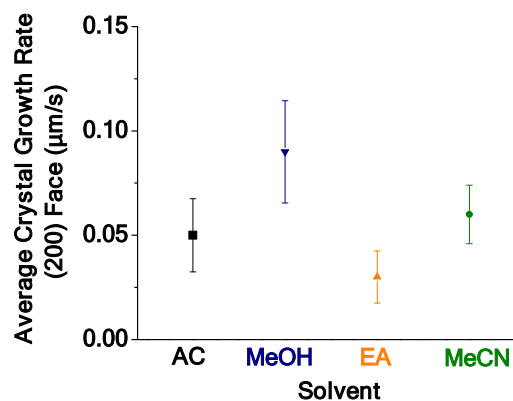
384 **Figure 8.** Average crystal growth rate of (a) length and (b) width ($\mu\text{m/s}$) of salicylamide seed
 385 crystals grown using the rotating disk method in four solvents (AC, MeCN, EA, MeOH) in
 386 temperature of 15 °C at supersaturation (S-1) of 0.03. Error bars are used to illustrate the
 387 standard deviation of the data.
 388

389 The (200) facet of salicylamide seed crystal grows faster in methanol compared to the
 390 other solvents, with acetonitrile and acetone having similar growth rates and lastly ethyl
 391 acetate with the slowest growth rates as shown in Figure 9. As methanol provided the
 392 fastest growth rates and ethyl acetate the slowest growth rates of the (200) facet, crystals grown
 393 in these two solvents are examined and SEM images are shown in Figure 10. The (200)
 394 surface of salicylamide crystals is more regular and structured when grown in MeOH than
 395 in EA. When examined in more detail the topographical features of the surface are
 396 different in the two solvents; when grown in MeOH the surface appears to have rows of
 397 steps whereas when grown in EA the surface is slightly different with a corrugated step
 398 appearance. It is known that the solvent may change the growth mechanism by way of the
 399 surface roughness³³⁻³⁴. The rows of steps may allow for easy lattice integration in
 400 comparison with the corrugated step surface and thus explain the difference in growth
 401 rates in the two solvents. These findings are in agreement with our previous work that found

1
2
3 402 ethyl acetate to have a stronger adsorption energy with salicylamide crystal facet than methanol

4 403 ³⁰.

5
6 404
7
8
9
10
11
12
13
14
15
16
17
18
19
20
21
22
23
24
25
26
27
28
29
30
31
32
33
34
35
36
37
38
39
40
41
42
43
44
45
46
47
48
49
50
51
52
53
54
55
56
57
58
59
60



405

406 **Figure 9.** Average crystal growth rate of (200) face ($\mu\text{m/s}$) under rotating disk conditions with
407 respect to four different solvents tested (200 rpm, 15 °C, 1 hr, S-1 of 0.03). Error bars are used
408 to illustrate the standard deviation of the data.

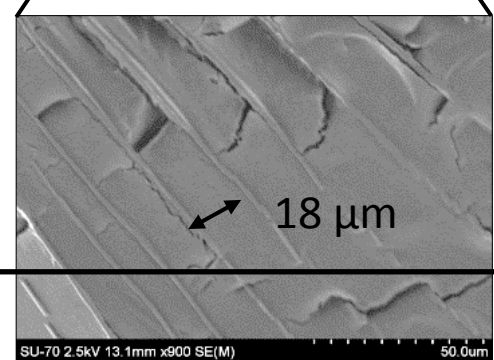
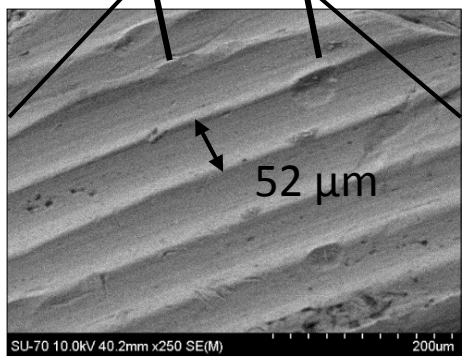
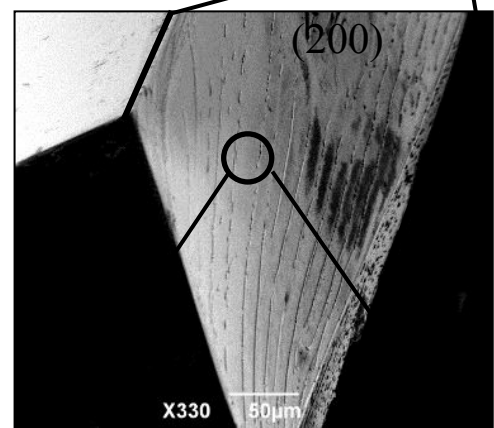
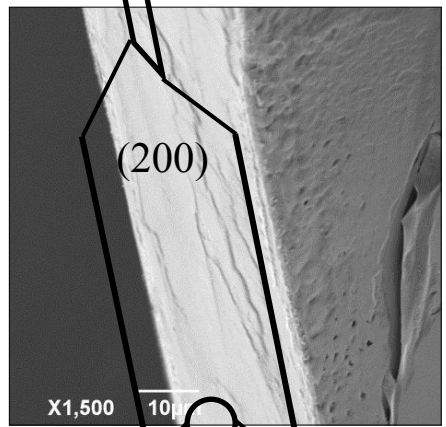
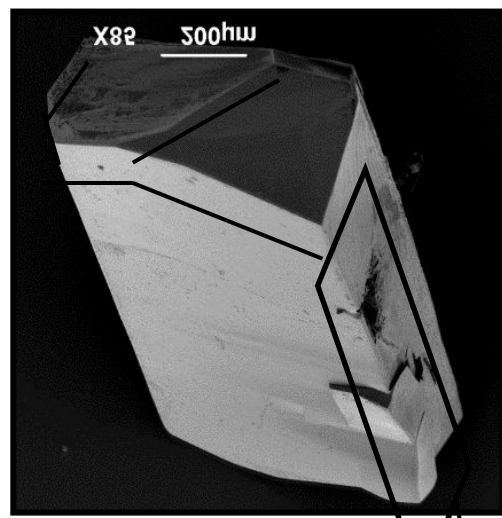
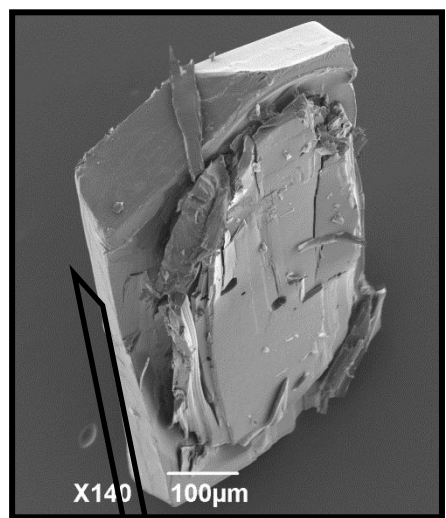
409

1
2
3 410
4
5
6 411
7
8 412
9
10
11 413
12
13 414
14
15 415
16
17 416
18
19 417
20
21 418
22
23
24 419
25
26 420
27
28 421
29
30 422
31
32 423
33
34 424
35
36 425
37
38 426
39
40 427
41
42 428
43
44 429
45
46 430
47
48 431
49
50
51 432
52
53
54
55
56
57
58
59
60

(200) Facet of Salicylamide

Ethyl Acetate

Methanol



1
2
3
4 433 **Figure 10.** SEM images of salicylamide crystals after growth via the rotating disk
5 434 method at 15 °C for 1 hr under S-1 of 0.03 in both EA and MeOH. The bottom two
6
7 435 SEM images show the topographical features of the (200) facet after growth in both
8
9 436 solvents.
10

11
12 437

13
14
15 438 *Kinetics – Effect of Supersaturation*

16
17 439 In general, increasing the driving force i.e. supersaturation leads to an increase in the
18
19 440 average crystal growth rates in both the length and width dimensions as shown in Figure
20
21 441 11. The extent of the increase in growth rate is dependant on the solvent; increasing
22
23 442 supersaturation (S-1) by 0.02 results in an increase in average growth of both length
24
25 443 and width directions by a factor of 2.0, 1.6, 1.5, and 3.5 in AC, MeCN, EA, and MeOH,
26
27 444 respectively. Methanol provides the largest increase in growth of salicylamide with
28
29 445 respect to same increase in supersaturation in the other solvents. The average growth
30
31 446 rate of the width direction in MeCN slightly decreases when increasing the
32
33 447 supersaturation (S-1) from 0.025 to 0.037. Yet the maximum growth rate of SAM
34
35 448 obtained in the lower and higher supersaturations were 0.19 $\mu\text{m/s}$ and 0.24 $\mu\text{m/s}$
36
37 449 respectively, proving that the higher driving force did in fact result in a higher growth
38
39 450 rate for some seed crystals. Interestingly in the case of acetonitrile were a relatively low
40
41 451 supersaturation of 0.012 was used, the average growth rate in both the length and width
42
43 452 dimension was negligible. However, upon visual examination of the crystals before and
44
45 453 after growth (Figure 12) under these conditions it is clear to see that a growth process
46
47 454 has occurred, primarily repairing morphological defects.
48

49 455
50
51
52
53
54
55
56
57
58
59
60

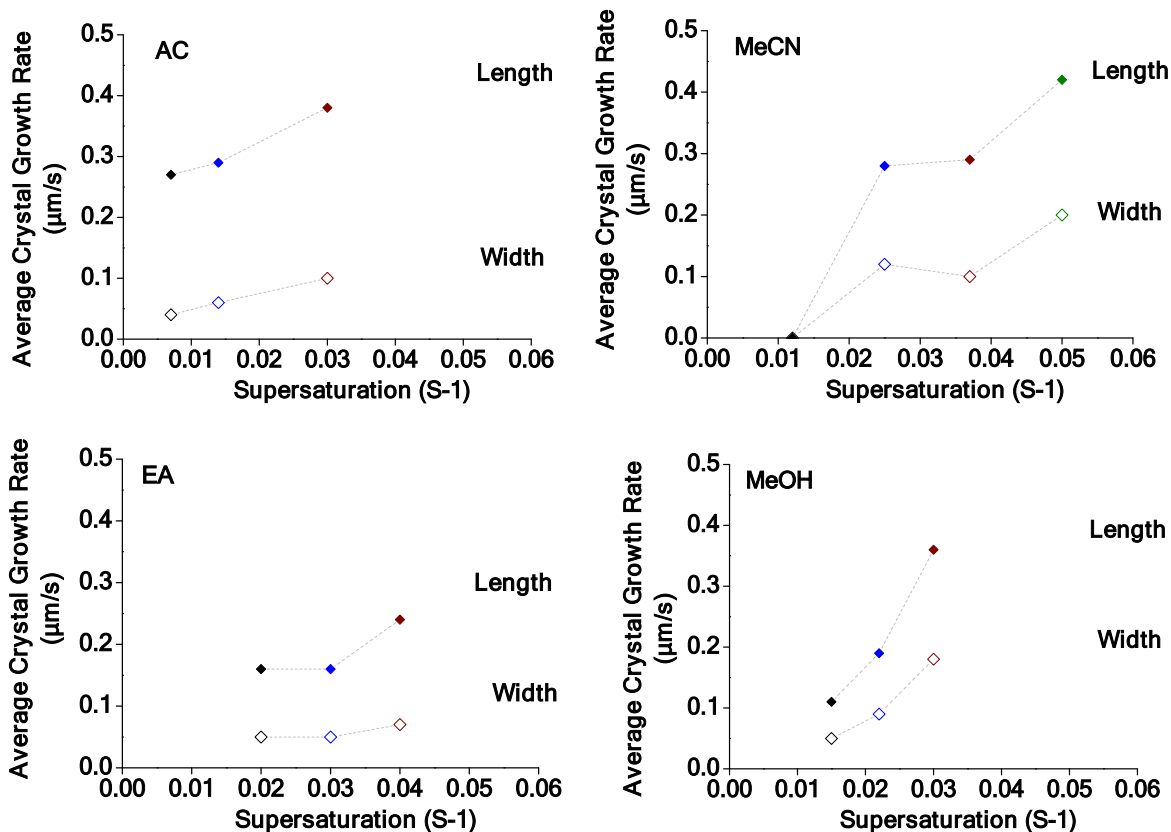


Figure 11. Average crystal growth rate ($\mu\text{m/s}$) of both length and width plotted against different supersaturations ($S-1$ of 0.007 to 0.05) for each of the four solvents.

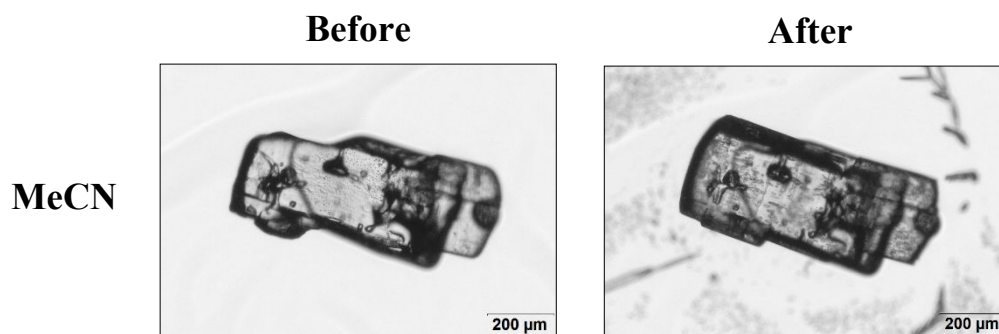


Figure 12. Micrographs show a salicylamide crystal before and after growth via the rotating disk method in acetonitrile at 15 $^{\circ}\text{C}$ for 1 hr at supersaturation ($S-1$) of 0.012.

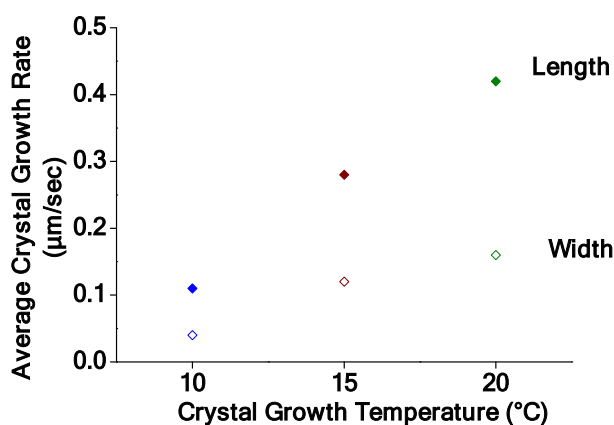
469 *Kinetics – Effect of Temperature*

470 The influence of temperature on the average crystal growth of salicylamide in
 471 acetonitrile is shown in Figure 13. A 10 °C increase in the temperature results in a
 472 fourfold increase in the average growth rate of SAM in the fastest growth direction,
 473 length. This strong dependence is of course reflected in the activation energies, E_a ,
 474 which can be obtained by fitting eq 3 to the average growth rates at the three
 475 temperatures, simultaneously. E_a values in the length and width directions are 93
 476 kJ/mol and 96 kJ/mol, respectively.

$$477 \quad G(s) = k_{g0} \exp\left(\frac{-E_a}{RT}\right) (S - 1)^g \quad (2)$$

$$478 \quad \ln G = \left(\frac{-E_a}{R}\right) \left(\frac{1}{T}\right) + \ln C \quad (3)$$

479 In our previous work ³², multiple salicylamide crystal seeds were grown in a batch
 480 reactor using an isothermal seeded desupersaturation crystal growth method.
 481 Increasing temperature within the same range from 10 °C to 20 °C in MeCN also led to
 482 a fourfold increase in the growth rate of salicylamide and the activation energy was
 483 found to be 96 kJ/mol. Despite significant differences between the two growth methods,
 484 it is of great reassurance that both methods estimate the same activation energy value.
 485 These activation energies are clearly higher than the values expected for simple
 486 molecular diffusion (5 – 20 kJmol⁻¹), and nearer those reported for surface integration
 487 (40 – 60 kJmol⁻¹)².



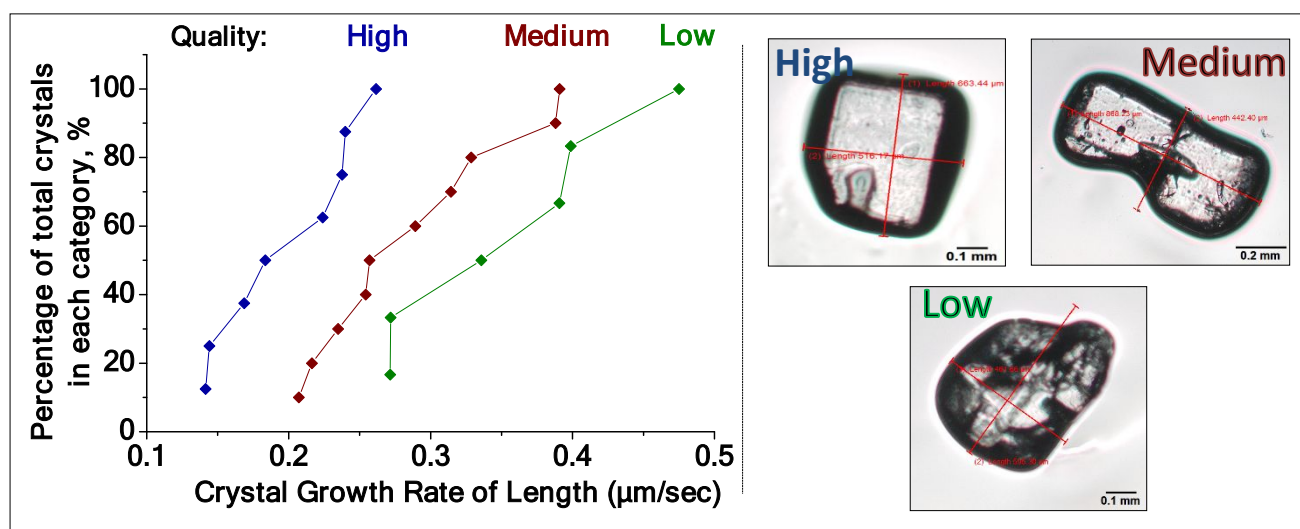
488

1
2
3
4 489 **Figure 13.** Average crystal growth rate ($\mu\text{m/s}$) of both length and width with respect to
5 490 the crystal growth temperature (10, 15, and 25 °C) for acetonitrile at initial
6
7 491 supersaturation ($S-1$) of 0.03 grown for 1 hr.
8
9

10 492
11
12
13
14
15
16
17
18
19
20
21
22
23
24
25
26
27
28
29
30
31
32
33
34
35
36
37
38
39
40
41
42
43
44
45
46
47
48
49
50
51
52
53
54
55
56
57
58
59
60

493 *Kinetics - Effect of the Crystal Seed Properties (Quality)*

494 As part of examining the influence of the properties of the seeds, the effect of the initial
 495 seed crystal quality was examined. For this purpose, the seed crystal quality is divided
 496 into three categories; “high” which refers to near perfect crystals in terms of symmetric
 497 shape and also surface, “medium” which refer to crystals that have an issue with shape
 498 or surface and lastly “low” which refer to crystals that have an issue with both the shape
 499 and crystal surface. An example of a seed crystal from each category is shown in Figure
 500 14. Initial seed crystal quality is found to have an impact on the crystal growth rate, with
 501 the “low” seed crystal quality leading to the fastest growth rates whereas “high” seed
 502 crystal quality having slower growth rates. This can be rationalised due to the increased
 503 number of surface defects present on the “low” quality crystals which can act as
 504 attachment sites for crystal growth units and so result in faster growth. Initial seed crystal
 505 quality plays a large effect on the growth rate dispersion (GRD) observed, a lower quality
 506 inherently results in wider GRD. There is an increase in the GRD by a factor of 2 for the “low”
 507 quality seed crystals versus the “high” quality seed crystal; 0.2 $\mu\text{m/s}$ range versus 0.1
 508 $\mu\text{m/s}$ range respectively. Industry require a narrow GRD and so using a high quality
 509 crystal seed would help in reducing it however at the pay-off of a reduced crystal growth
 510 rate.



1
2
3 512 **Figure 14.** Comparing crystal growth rate of length ($\mu\text{m/s}$) of salicylamide in acetonitrile with
4 513 respect to initial seed crystal quality (high, medium and low). On the right hand side of the
5 514 figure are examples of a seed crystal from each of the crystal quality categories for clarity.
6
7

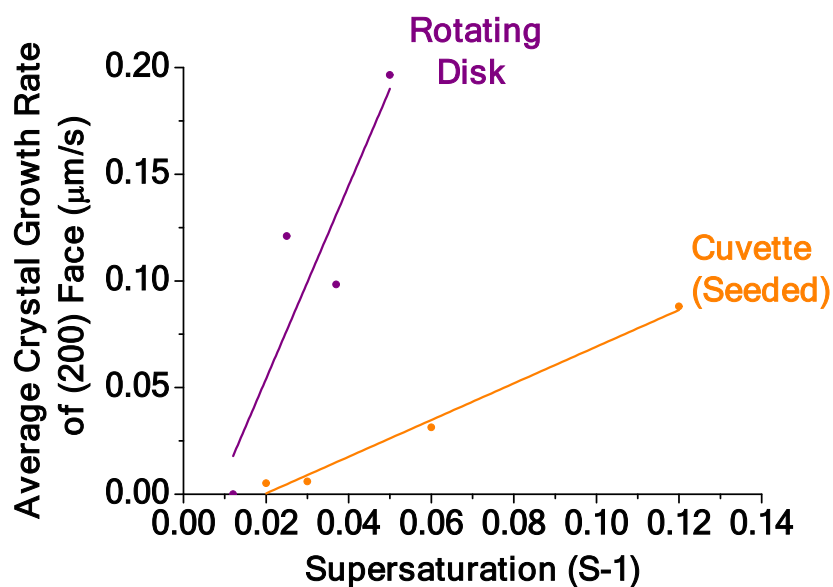
8 515
9
10
11
12
13
14
15
16
17
18
19
20
21
22
23
24
25
26
27
28
29
30
31
32
33
34
35
36
37
38
39
40
41
42
43
44
45
46
47
48
49
50
51
52
53
54
55
56
57
58
59
60

516 Comparison of growth rates obtained from the two crystal growth methods

517 Salicylamide seed crystal growth rates obtained from the cuvette and the rotating disk
 518 experiments at 15 °C are compared in Figure 15. The cuvette growth experiments are performed
 519 without forced convection whereas in the rotating disk experiments there is a fairly controlled
 520 hydrodynamic situation in the rotation of the disk at 200 rpm. Obviously the growth rate is much
 521 higher in the rotating disc experiments, e.g. at (S-1) of 0.03 the average growth increases by a
 522 factor of 20 (0.003 $\mu\text{m/s}$ versus 0.060 $\mu\text{m/s}$) for cuvette growth method and the rotating disk
 523 method respectively.

524 Crystal growth is widely accepted to occur by two phenomena assumed to act in series; transport
 525 of solute through the liquid boundary layer to the crystal-liquid interface (volume diffusion) and
 526 integration of solute molecules into the crystal lattice (surface integration)^{1-2, 35-37}. With
 527 increasing relative velocity between the crystals and the fluid the volume diffusion resistance
 528 decreases. The crystal growth rate increases and the crystal growth process becomes increasingly
 529 governed by the surface integration step. Accordingly, it is perfectly in accordance with
 530 expectation that the cuvette experiments would deliver a growth rate that is equal to or lower
 531 than the rotating disc growth rates⁶. The fact that there is a substantial difference reveals that at
 532 least the cuvette experiments are significantly influenced by the volume diffusion resistance.

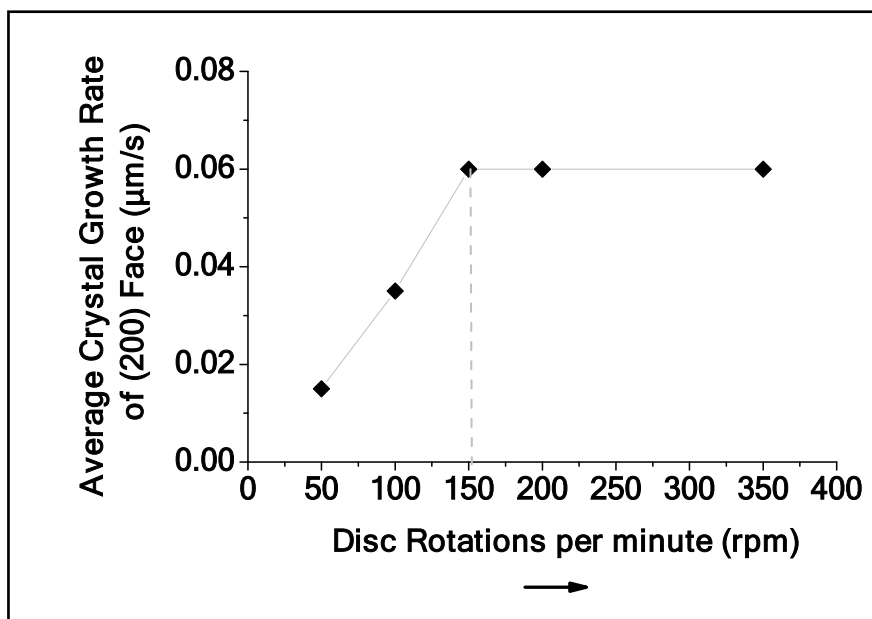
533 The influence of the rotation rate from 50 rpm up to 350 rpm has been evaluated for crystal
 534 growth in acetonitrile and the result is illustrated in Figure 16. Above 150 rpm the growth rate
 535 no longer increases with increasing rotation rate. Accordingly, a stirring speed of 150 rpm is
 536 found to be sufficient to essentially eliminate the volume diffusion mass transfer resistance, and
 537 accordingly the growth experiments performed at 200 rpm can be assumed to be governed by
 538 surface integration.



539

540 **Figure 15.** Average crystal growth rate ($\mu\text{m/s}$) of the (200) face of salicylamide seed crystals
 541 grown in acetonitrile in supersaturation (S-1) range of 0.01 – 0.12 at 15 °C by the two crystal

1
2
3 542 growth methods outlined in this paper. The cuvette growth method is shown as the orange
4 543 triangles and the rotating disk growth method is shown as the purple circles.



26 544
27 545 **Figure 16.** Average crystal growth rate ($\mu\text{m/s}$) of the (200) face of salicylamide seed crystals
28 546 grown using the rotating disk growth method at different stirring rates (50 to 350 rpm) in
29 547 acetonitrile with supersaturation ($S-1$) of 0.03 at 15 °C.

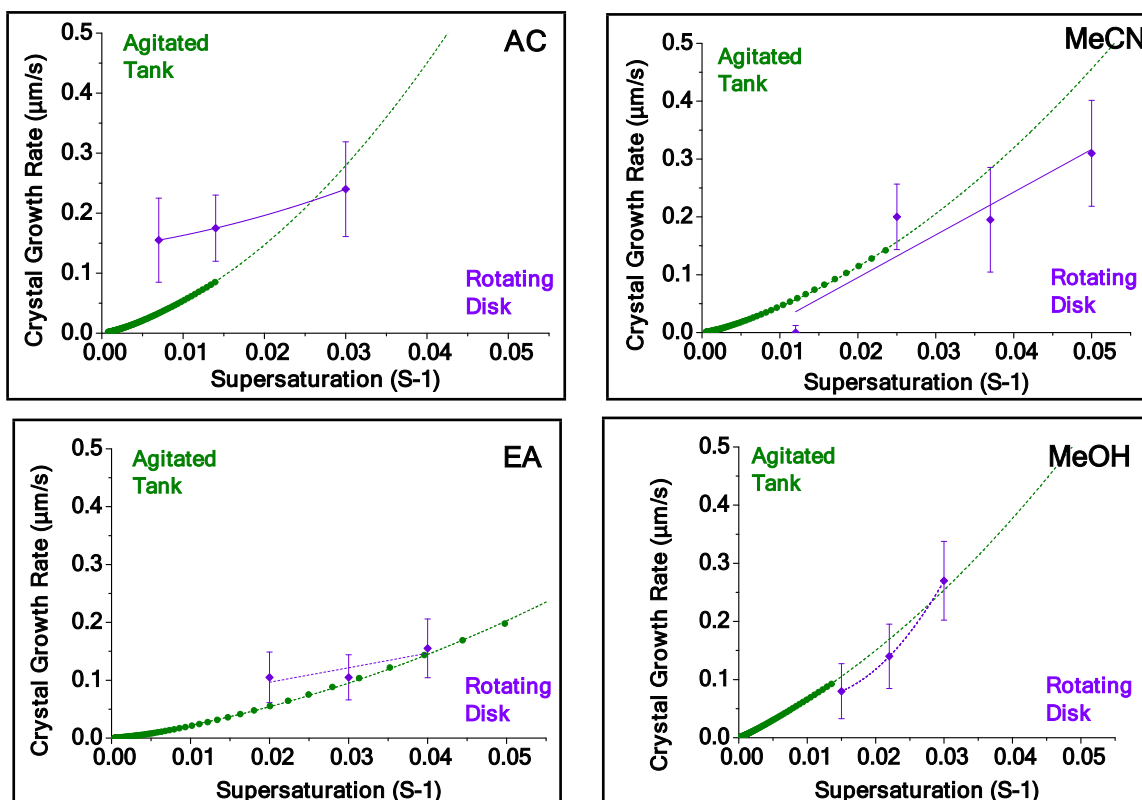
1
2
3
4 549 Comparison of rotating disk crystal growth with previously published crystal growth
5
6 550 studies

7
8 551 In our previous work ³², a batch agitated reactor was used to grow multiple salicylamide seed
9 552 crystals via a seeded isothermal desupersaturation crystal growth method. This study used the
10 553 exact same sieve fraction 300 – 355 μm and solvents as were used in the rotating disk study, and
11 554 the same crystal growth temperature and similar supersaturation range. The growth order
12 555 parameter indicated that the growth process in the batch reactor was governed by surface
13 556 integration. In Figure 18, these results are compared with the present rotating disk results. In all
14 557 solvents, the magnitude of growth in the two methods is the same. In MeCN, EA and MeOH the
15 558 growth rates are very similar, whereas in AC the growth is slightly faster in the rotating disk
16 559 experiments. The slight variations in growth rates can be explained by the differences in the
17 560 number of crystals involved; on average 12,000 crystals are grown simultaneously in the batch
18 561 crystal growth study whereas the rotating disk studies only 32 crystals are grown at the same
19 562 time. This paper has shown that the growth rate dispersion for salicylamide crystal growth data
20 563 is relatively wide, hence the larger sample size in the agitated reactor experiments would lead to
21 564 better estimation of the average crystal growth rate. In addition, it should be recognised that in
22 565 the rotating disk method the growth in a specific direction for each crystal is directly measured
23 566 as an increase in the linear dimension, whereas in the batch reactor method the overall average
24 567 growth rate in terms of the linear dimension used to characterise the size over all crystals is
25 568 determined indirectly by recording the decay in solution concentration and assuming a constant
26 569 crystal shape. Accordingly, the two methods have different merits and drawbacks and
27 570 complement one another, and the overall agreement is encouraging.

28
29
30
31
32
33
34
35 571
36
37
38
39
40
41
42
43
44
45
46
47
48
49
50
51
52
53
54
55
56
57
58
59
60

572

573



574 **Figure 17.** Crystal growth rate of salicylamide crystals grown by two methods in the
575 four solvents at 15 °C with respect to supersaturation. The crystal growth rate (µm/s)
576 for the rotating disk studies is equal to the average growth rate of length plus the
577 average growth rate of width divided by two. The agitated tank crystal growth rates are
578 obtained from our previous study ³².

579

580

581

582 **Conclusion**

583 Crystal growth of salicylamide was investigated under both diffusion and surface
584 integration control, and the associated growth rates were measured. The crystal growth
585 rates of the (200) facet obtained under surface integration controlled growth resulted in
586 20 times faster growth rates than when grown under diffusion controlled growth. Under
587 surface integration controlled growth process, when salicylamide was grown in MeOH
588 the surface appeared to have rows of steps whereas when it was grown in EA the
589 surface was comprised of a corrugated step appearance. Within acetonitrile, increasing
590 temperature by 10°C led to a fourfold increase in salicylamide's growth rates in the
591 length direction. The rotating disk method delivered growth rates in good agreement
592 with our previous data obtained by isothermal seeded desupersaturation experiments
593 in an agitated tank. The rotating disk method allows for a more detailed examination of
594 the growth in particular directions and of particular faces, while simultaneously allowing
595 for data of a number of crystals to be collected simultaneously. By changing the rotation
596 rate the relative influence of boundary layer diffusion can be changed, and in the
597 presented work 200 rpm was sufficient to have full surface integration control.

599 **Supporting Information**

600 The supporting information is available free of charge on the ACS Publications website at DOI:
601 #####.

602 Supporting information for the rotating disk studies can be found including experimental
603 supersaturation decay, testing reproducibility of the method, effect of crystal number/ position
604 on disk and effect of growth time on the rotating disk method.

605 **Author Information**

606 Corresponding Author

607 *E-mail: Ake.Rasmuson@ul.ie

608 Notes

609 The authors declare no competing financial interest.

610

611 Acknowledgments

612 This publication has emanated from research conducted with the financial support of
613 the Synthesis and Solid State Pharmaceutical Centre (SSPC), financed by a research
614 grant from Science Foundation Ireland (SFI) co-funded under the European Regional
615 Development Fund (Grant Number 12/RC/2275).

616 References

- 617 1. MERSMANN, A., *Crystallization Technology Handbook*. M. Dekker: New York,
618 1995; p 1513-1514.
- 619 2. Lacmann, R., *Crystallization*, Third Edition. J. W. MULLIN, Butterworth-Heinemann,
620 Oxford 1997, 527 Seiten, zahlr. Abb. und ISBN 0-7506-3759-5. *Chemie Ingenieur Technik*
621 **1998**, 70 (11), 1468-1468.
- 622 3. Wu, K.; Ma, C. Y.; Liu, J. J.; Zhang, Y.; Wang, X. Z., Measurement of Crystal Face
623 Specific Growth Kinetics. *Crystal Growth & Design* **2016**, 16 (9), 4855-4868.
- 624 4. Perry, A. R.; Peruffo, M.; Unwin, P. R., Quantitative Plane-Resolved Crystal Growth
625 and Dissolution Kinetics by Coupling In Situ Optical Microscopy and Diffusion Models: The
626 Case of Salicylic Acid in Aqueous Solution. *Crystal Growth & Design* **2013**, 13 (2), 614-622.
- 627 5. Cano, H.; Gabas, N.; Canselier, J. P., Experimental study on the ibuprofen crystal
628 growth morphology in solution. *Journal of Crystal Growth* **2001**, 224 (3-4), 335-341.
- 629 6. Land, T. A.; De Yoreo, J. J.; Lee, J. D., An in-situ AFM investigation of canavalin
630 crystallization kinetics. *Surface Science* **1997**, 384 (1), 136-155.
- 631 7. Kitamura, M.; Onuma, K., In Situ Observation of Growth Process of α -L-Glutamic
632 Acid with Atomic Force Microscopy. *Journal of Colloid and Interface Science* **2000**, 224 (2),
633 311-316.
- 634 8. Hottenhuis, M. H. J.; Lucasius, C. B., The influence of impurities on crystal growth; In
635 situ observation of the {010} face of potassium hydrogen phthalate. *Journal of Crystal Growth*
636 **1986**, 78 (2), 379-388.
- 637 9. Zhang, R.; Ma, C. Y.; Liu, J. J.; Zhang, Y.; Liu, Y. J.; Wang, X. Z., Stereo imaging
638 camera model for 3D shape reconstruction of complex crystals and estimation of facet growth
639 kinetics. *Chemical Engineering Science* **2017**, 160, 171-182.
- 640 10. Davey, R. J.; Mullin, J. W., Growth of the {100} faces of ammonium dihydrogen
641 phosphate crystals in the presence of ionic species. *Journal of Crystal Growth* **1974**, 26 (1), 45-
642 51.
- 643 11. Li, L.; Rodríguez-Hornedo, N., Growth kinetics and mechanism of glycine crystals.
644 *Journal of Crystal Growth* **1992**, 121 (1), 33-38.

- 1
2
3 645 12. Pfeiffer, H., Analytical Theory of the Growth of Crystal Faces. *physica status solidi (a)*
4 646 **1983**, 79 (2), 445-454.
- 5 647 13. Borchert, C.; Temmel, E.; Eisenschmidt, H.; Lorenz, H.; Seidel-Morgenstern, A.;
6 648 Sundmacher, K., Image-Based in Situ Identification of Face Specific Crystal Growth Rates
7 649 from Crystal Populations. *Crystal Growth & Design* **2014**, 14 (3), 952-971.
- 8 650 14. Nguyen, T. T. H., R. B.; Roberts, K. J.; Marziano, I.; Nichols, G., Precision
9 651 measurement of the growth rate and mechanism of ibuprofen {001} and {011} as a function of
10 652 crystallization environment. *CrystEngComm* **2014**, 16 (21), 4568-4586.
- 11 653 15. Bentivoglio, M., An investigation of the rate of growth of crystals in different
12 654 directions. *Proc. R. Soc. Lond. A* **1927**, 115 (770), 59-87.
- 13 655 16. Beckmann, W., Simultaneous measurement of the growth rates of the (001) and (110)
14 656 faces of stearic acid growing from solution. *Journal of Physics E: Scientific Instruments* **1986**,
15 657 19 (6), 444.
- 16 658 17. Kitamura, M.; Ishizu, T., Growth kinetics and morphological change of polymorphs of
17 659 L-glutamic acid. *Journal of Crystal Growth* **2000**, 209 (1), 138-145.
- 18 660 18. Schram, C. J.; Smyth, R. J.; Taylor, L. S.; Beaudoin, S. P., Understanding Crystal
19 661 Growth Kinetics in the Absence and Presence of a Polymer Using a Rotating Disk Apparatus.
20 662 *Crystal Growth & Design* **2016**, 16 (5), 2640-2645.
- 21 663 19. Bourne, J. R.; Davey, R. J.; Gros, H.; Hungerbühler, K., The rotating disc configuration
22 664 in the measurement of crystal growth kinetics from solution. *Journal of Crystal Growth* **1976**,
23 665 34 (2), 221-229.
- 24 666 20. Wang, X. Z.; Calderon De Anda, J.; Roberts, K. J., Real-Time Measurement of the
25 667 Growth Rates of Individual Crystal Facets Using Imaging and Image Analysis. *Chemical*
26 668 *Engineering Research and Design* **2007**, 85 (7), 921-927.
- 27 669 21. Ma, C. Y.; Wang, X. Z., Model identification of crystal facet growth kinetics in
28 670 morphological population balance modeling of l-glutamic acid crystallization and experimental
29 671 validation. *Chemical Engineering Science* **2012**, 70, 22-30.
- 30 672 22. Johnstone, R. D. L.,; Lennie, A. R.,; Parker, S. F.,; Parsons, S.,;Pidcock,
31 673 E.,;Richardson, P. R.,;Warren, J. E.,;Wood, P. A., High-pressure polymorphism in
32 674 salicylamide. *CrystEngComm* **2010**, 12 (4), 1065-1078.
- 33 675 23. Nordstrom, F. L.; Svard, M.; Rasmuson, A. C., Primary nucleation of salicylamide: the
34 676 influence of process conditions and solvent on the metastable zone width. *CrystEngComm*
35 677 **2013**, 15 (36), 7285-7297.
- 36 678 24. Nordström, F., L.,; Rasmuson, Å. C., Solubility and Melting Properties of Salicylamide.
37 679 *J. Chem. Eng. Data* **2006**, 51 (5), 1775-1777.
- 38 680 25. Sankaranarayanan, K.; Ramasamy, P., Unidirectional seeded single crystal growth from
39 681 solution of benzophenone. *Journal of Crystal Growth* **2005**, 280 (3-4), 467-473.
- 40 682 26. El-Zhry El-Yafi, A. K.; El-Zein, H., Technical crystallization for application in
41 683 pharmaceutical material engineering: Review article. *Asian Journal of Pharmaceutical*
42 684 *Sciences* **2015**, 10 (4), 283-291.
- 43 685 27. Demazeau, G., Review. Solvothermal Processes: Definition, Key Factors Governing the
44 686 Involved Chemical Reactions and New Trends. In *Zeitschrift für Naturforschung B*, 2010; Vol.
45 687 65, p 999.
- 46 688 28. Online, K. L., Tables of Physical & Chemical Constants (16th edition 1995). In 2.2.3
47 689 *Viscosities* [Online] 2005. www.kayelaby.npl.co.uk.
- 48 690 29. Wilke, C. R.; Chang, P., Correlation of diffusion coefficients in dilute solutions. *AIChE*
49 691 *Journal* **1955**, 1 (2), 264-270.
- 50 692 30. Lynch, A.; Verma, V.; Zeglinski, J.; Bannigan, P.; Rasmuson, Å., Face indexing and
51 693 shape analysis of salicylamide crystals grown in different solvents. *CrystEngComm* **2019**.
- 52
53
54
55
56
57
58
59
60

- 1
2
3 694 31. Dowling, R.; Davey, R. J.; Curtis, R. A.; Han, G.; Poornachary, S. K.; Chow, P. S.;
4 695 Tan, R. B. H., Acceleration of crystal growth rates: an unexpected effect of tailor-made
5 696 additives. *Chemical Communications* **2010**, *46* (32), 5924-5926.
6 697 32. Lynch, A.; Jia, L.; Svärd, M.; Rasmuson, Å. C., Crystal Growth of Salicylamide in
7 698 Organic Solvents. *Crystal Growth & Design* **2018**, *18* (12), 7305-7315.
8 699 33. Beckmann, W., *Crystallization: Basic Concepts and Industrial Applications*. Wiley:
9 700 2013.
10 701 34. J. Davey, R.; Milisavljevic, B.; R. Bourne, J., *Solvent interactions at crystal surfaces:*
11 702 *the kinetic story of .alpha.-resorcinol*. 1988; Vol. 92.
12 703 35. Humphreys-Owen, S. P. F., Crystal Growth from Solution. *Proceedings of the Royal*
13 704 *Society of London. Series A, Mathematical and Physical Sciences* **1949**, *197* (1049), 218-237.
14 705 36. Bennema, P., The importance of surface diffusion for crystal growth from solution.
15 706 *Journal of Crystal Growth* **1969**, *5* (1), 29-43.
16 707 37. Chen, J., ; Sarma, B.; Evans, J. M. B.,; Myerson, A. S., Pharmaceutical Crystallization.
17 708 *Cryst. Growth Des.* **2011**, *11* (4), 887-895.

21 709

24 710

711

For Table of Contents Use Only

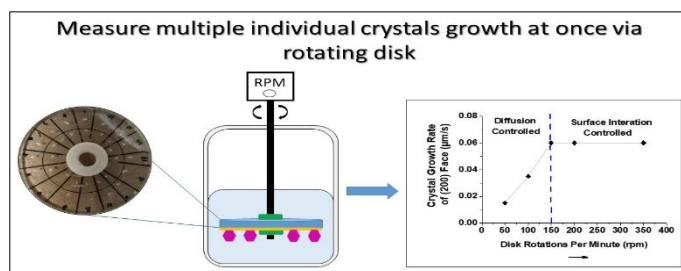
712

Crystal Growth of Single Salicylamide Crystals

713

Lynch Aisling¹, Rasmuson Åke^{1,2}*

714



715